Analysis of Discontinuity Induced Bifurcations in a Dual Input DC-DC Converter

Damian Giaouris
Chemical Process Engineering Research Institute, Centre for Research and Technology, Hellas, Thermi-Thessaloniki, Greece

Soumitro Banerjee, Kuntal Mandal
Department of Physical Sciences, Indian Institute of Science Education and Research - Kolkata, Mohanpur Campus - 741252, West Bengal, India
Department of Electrical and Computer Engineering, College of Engineering, King Abdulaziz University, Jeddah, Saudi Arabia

Mohammed M. Al-Hindawi, Abdullah Abusorrah, Yusuf Al-Turki
Department of Electrical and Computer Engineering, College of Engineering and Renewable Energy Research Group, King Abdulaziz University, Jeddah, Saudi Arabia

Abdelali El Aroudi
GAEI research group, Dept. d'Enginyeria Electrònica, Elèctrica i Automàtica, Universitat Rovira i Virgili, 43007, Tarragona, Spain

Received (to be inserted by publisher)

DC-DC power converters with multiple inputs and a single output are used in numerous applications where multiple sources, e.g., two or more renewable energy sources and/or a battery, feed a single load. In this work a classical boost converter topology with two input branches connected to two different sources is chosen, with each branch independently being controlled by a separate peak current mode controller. We demonstrate for the first time that even though this converter is similar to other well known topologies that have been studied before, it exhibits many complex nonlinear behaviours that are not found in any other standard PWM controlled power converter. The system undergoes period incrementing cascade as a parameter is varied, with discontinuous hard transitions between consecutive periodicities. We show that the system can be described by a discontinuous map, which explains the observed bifurcation phenomena. The results have been experimentally validated.

Keywords: Dual input converters, bifurcation, discontinuous map

1. Introduction

Power converters form an essential part of almost all electrical equipment, from simple domestic appliances to laptops, electrical vehicles, airplanes and others [Kassakian *et al.*, 1991]. The basic task of such electronic systems is to connect different types of power supplies to various loads that operate at different voltage and/or current levels under varying operating conditions. As the parameters external to the converter (like the input voltage or the load) are varied, the converter may become unstable exhibiting subharmonic or slow-timescale oscillations which are caused by the essential nonlinearity of the switching action. These

instabilities are due to various smooth/nonsmooth bifurcations and have attracted a lot of interest [Banerjee & Verghese, 2001; Tse, 2003; di Bernardo *et al.*, 2008; Kuznetsov, 2004; Zhusubaliyev & Mosekilde, 2003; El Aroudi *et al.*, 2010; Spinu *et al.*, 2012]. Traditionally, the averaged model is used to design and study such systems [Tse, 2003], but this approach cannot predict fast-scale bifurcations [Banerjee & Chakrabarty, 1998] and border collisions [Yuan *et al.*, 1998]. On the other hand, it has been shown that the sampled data model [Kassakian *et al.*, 1991] or the Poincaré map [Hamill & Deane, 1992] can predict such behavior and therefore it is preferred when a thorough analysis of the converter is required. For most power electronic converters this Poincaré map turns out to be non-smooth, but continuous [Zhao *et al.*, 2009]. Discontinuous maps have so far been used in rare occasions; for example to model power electronic systems with pulse-skipping modulation [Kapat *et al.*, 2010] or when nonidealities like switching delay become significant [Banerjee *et al.*, 2005]. Such maps also have been used to model induction motor drives with Direct Torque Control [Suto *et al.*, 2009]. In all cases one-dimensional (or at most 2-dimensional) discontinuous maps sufficed in describing the system dynamics with reasonable accuracy, and the theory for such maps is available [Jain & Banerjee, 2003; Rakshit *et al.*, 2010].

In this paper we consider a boost power converter that receives supply from two different sources and delivers regulated power to a single load [Xiong *et al.*, 2013; Ohata & Saito, 2013; Zhou *et al.*, 2012]. It is possible to apply various control strategies in such systems (like interleaving operation [Van der Broeck & Tezcan, 2006]) but in this work it was decided to have independent control of the currents drawn from the two sources, and additionally regulate the output voltage. Such converters are needed in distributed generation systems, especially in renewable energy technologies as well as energy harvesting applications [Shi *et al.*, 2011]. Even though this is another type of the well studied power converter topologies, it shows a wide variety of interesting results that cannot be explained using the available theory for continuous non-smooth maps. In order to overcome this problem, we derive the discrete-time model and demonstrate that it is not only nonlinear or non-smooth, but is also discontinuous. The resulted map differs from the aforementioned 1D and 2D cases as now 3 dimensions are required in order to describe the system. Therefore, apart from presenting the nonlinear phenomena in a practical dc-dc converter, this work also serves as a motivating case study showing the necessity of developing a theory for high order discontinuous maps.

This paper is structured as follows. In Section 2 the basic converter topology and control strategy are described and the desired operation is shown through various time domain responses. This is then followed by a motivating example in which the period-1 orbit loses stability through a discontinuous border collision bifurcation. In Section 3 the mathematical model of the converter is developed and the Poincaré map is derived by considering all possible switching sequences in one clock cycle. In section 4 we present the full nonlinear behaviour of the system and its bifurcation analysis. Finally in section 5 we experimentally validate our findings.

2. System Description

The dual-input boost converter considered in this study is shown in Fig. 1, [Zhou *et al.*, 2012]. The first phase is controlled by a peak current mode controller where the demanded current I_{ref1} can be set independently, and the second phase is controlled by another peak current mode controller with an outer voltage feedback loop that sets the reference current I_{ref2}. That way the dc component of the output voltage remains fixed regardless of the current drawn from the first phase which can be adjusted in order to implement a specific power management strategy (for example, the supply of the first phase may be a battery which we do not want to deplete). At this point it has to be mentioned that in practical applications, a ramp compensator would have been added to the two peak current controllers and a PI controller instead of a simple proportional one would have been employed for the control of the output voltage. Our simulations indicated that the insertion of the ramp compensator and the usage of the integral-term do not qualitatively change the behaviour of the system. Therefore in order to simplify the analysis we chose not to use them. Having said that, care has to be taken here, as in [Giaouris *et al.*, 2012] and [Chen *et al.*, 2007] it has been shown that under a wrong parameter choice it is possible to have interaction of a fast- and a slow-timescale oscillations.

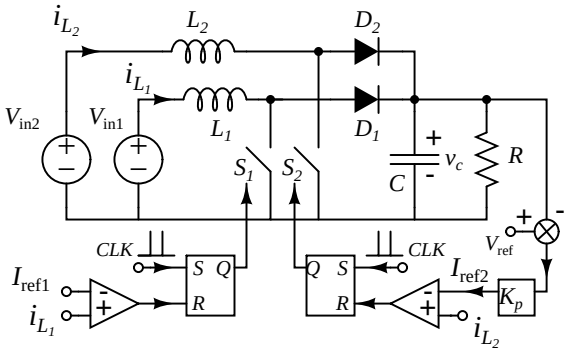

Fig. 1. Schematic diagram of a dual input boost converter and its control.

The parameters of the converter were specifically chosen to be identical to those used in other publications [Tse, 2003] in order to be able to highlight the differences that occur when a second phase is added. Fig. 2 shows the response of the converter for two different values of the demanded current I_{ref1} in the first phase and we see that while the output voltage remains more or less constant (with a small ripple), the output current of the second phase is adjusted according to the demanded current of the first phase. This mode of operation is commonly called period-1 as all the state variables oscillate with period T. However if we further increase the demanded current of the first phase, the operation suddenly changes to period-11 at $I_{\text{ref1}} = 0.36$ A, as shown in Fig. 3. Apart from this sudden transition to a high periodic orbit, we also observe that the output voltage at some points becomes less than V_{in1} and/or V_{in2}. The bifurcation diagram is presented in Fig. 4, from which two critical observations can be made: a) there is a sudden transition from a period-1 orbit to period-11 orbit and b) after this first bifurcation takes place, there is a sequence of bifurcations where the periodicity increases or decreases by 1. As it will be shown later, these peculiar bifurcation phenomena are caused by the fact that the Poincaré map of the system is discontinuous [Jain & Banerjee, 2003; Rakshit *et al.*, 2010].

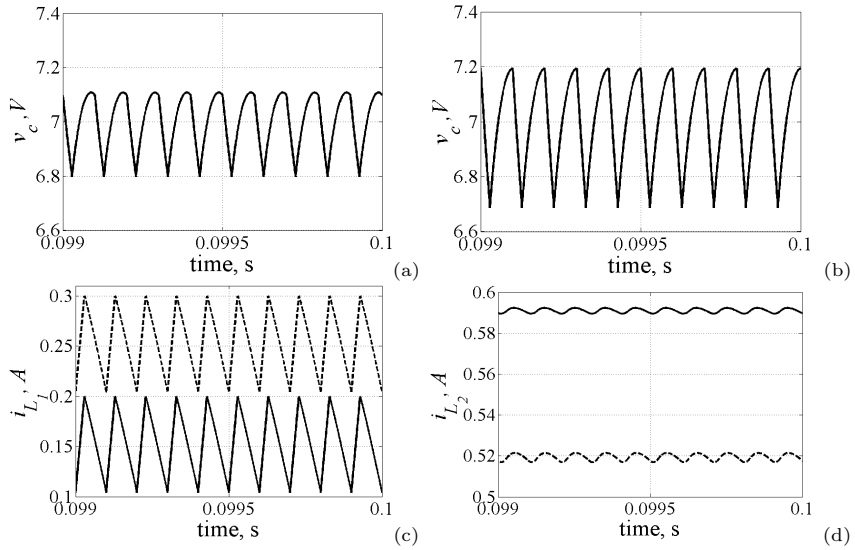

Fig. 2. Responses of the system for (a) $I_{\text{ref1}} = 0.2$ A and (b) $I_{\text{ref1}} = 0.3$ A; (c) and (d) show the currents in the two branches (firm line for $I_{\text{ref1}} = 0.2$ A and dashed line for $I_{\text{ref1}} = 0.3$ A). The rest of the parameters are $V_{\text{in1}} = 5$ V, $L_1 = L_2 = 1.5$ mH, $C = 10$ μF, $R = 10$ Ω, $T = 100$ μs, $V_{\text{ref}} = 12$ V, $K_p = 0.1$, $V_{\text{in2}} = 7$ V.

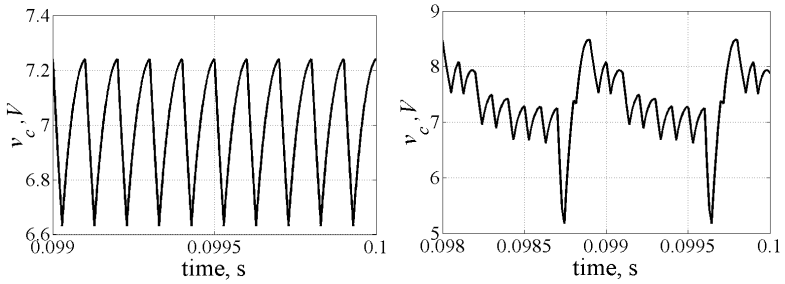

Fig. 3. Voltage responses for $I_{\text{ref1}} = 0.35$ A (left): period-1 and $I_{\text{ref1}} = 0.36$ A (right): period-11.

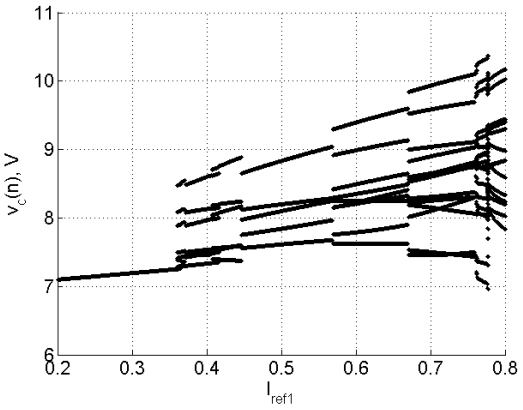

Fig. 4. Bifurcation diagram for variation of I_{ref1}, with $V_{\text{in1}} = 5$ V, $V_{\text{in2}} = 7$ V, $V_{\text{ref}} = 12$ V.

3. Mathematical Modeling

Assuming ideal components, the system can be described by a set of ODEs that form a piecewise smooth model, given by

$$\frac{d\boldsymbol{x}}{dt} = \boldsymbol{A}(s_1, s_2)\, \boldsymbol{x} + \boldsymbol{B}$$

where

$$\boldsymbol{x} = \begin{bmatrix} v_c \\ i_{L_1} \\ i_{L_2} \end{bmatrix},\ \boldsymbol{B} = \begin{bmatrix} 0 \\ \frac{V_{\text{in1}}}{L_1} \\ \frac{V_{\text{in2}}}{L_2} \end{bmatrix},\ \mathbf{A} = \begin{bmatrix} \frac{-1}{RC} & \frac{\bar{s}_1}{C} & \frac{\bar{s}_2}{C} \\ \frac{-\bar{s}_1}{L_1} & 0 & 0 \\ \frac{-\bar{s}_2}{L_2} & 0 & 0 \end{bmatrix}$$

Here s_1, s_2 are the binary control signals of the two switches, and $\bar{s}_1 = 1 - s_1$ and $\bar{s}_2 = 1 - s_2$. The control of the two switches is governed by the following scalar functions

$$\text{for } S_1 : h_1(\boldsymbol{x}) = x_2 - I_{\text{ref1}}$$
$$\text{for } S_2 : h_2(\boldsymbol{x}) = x_3 - I_{\text{ref2}} = x_3 - K_p(V_{\text{ref}} - x_1)$$

At the beginning of a clock cycle, the two switches can have the states 0 or 1. Thus there are 4 possible combinations. Similarly at the end of a clock cycle there are 4 possible combinations. This gives 16 possible ways of transiting from the beginning to the end of a clock cycle. But out of these 7 can be ignored because if a switch is OFF at the start of a clock cycle it remains OFF for the whole period. Table 1 shows these possible combinations.

It has to be noted here that the case $(1,1) \to (0,0)$ can be achieved in 3 different ways:

- $(1,1) \to (0,0)$, both switches change at the same instant
- $(1,1) \to (1,0) \to (0,0)$, S_2 changes its state before S_1
- $(1,1) \to (0,1) \to (0,0)$, S_1 changes its state before S_2

$(1,1) \to (1,1)$	~~$(1,0) \to (1,1)$~~	~~$(0,1) \to (1,1)$~~	~~$(0,0) \to (1,1)$~~
$(1,1) \to (1,0)$	$(1,0) \to (1,0)$	~~$(0,1) \to (1,0)$~~	~~$(0,0) \to (1,0)$~~
$(1,1) \to (0,1)$	~~$(1,0) \to (0,1)$~~	$(0,1) \to (0,1)$	~~$(0,0) \to (0,1)$~~
$(1,1) \to (0,0)$	$(1,0) \to (0,0)$	$(0,1) \to (0,0)$	~~$(0,0) \to (0,0)$~~

As the vector fields before and after each switching are linear, the evolution between two switching instances, t_1 and t_2, is given by:

$$\boldsymbol{x}(t_2) = e^{\boldsymbol{A}(s_1,s_2)(t_2-t_1)}\boldsymbol{x}(t_1) + \int_{t_1}^{t_2} e^{\boldsymbol{A}(s_1,s_2)(t_2-\tau)}\boldsymbol{B}d\tau.$$

Therefore, by defining

$$\boldsymbol{\Phi}(s_1,s_2,t_1,t_2) = e^{\boldsymbol{A}(s_1,s_2)(t_2-t_1)}, \boldsymbol{I}(s_1,s_2,t_1,t_2) = \int_{t_1}^{t_2} e^{\boldsymbol{A}(s_1,s_2)(t_2-\tau)}\boldsymbol{B}d\tau,$$

the 10 possible evolutions in a clock cycle (i.e., the Poincaré maps) are:

$$(s_1,s_2) \to (s_1,s_2) : \boldsymbol{x}(T) = \boldsymbol{\Phi}(s_1,s_2,0,T)\boldsymbol{x}(0) + \boldsymbol{I}(s_1,s_2,0,T),$$

with $s_1, s_2 \in \{0,1\} \times \{0,1\}$.

$$\begin{aligned}
(s_1,1) \to (s_1,0): \quad \boldsymbol{x}(T) &= \boldsymbol{\Phi}(s_1,0,d_2T,T)((\boldsymbol{\Phi}(s_1,1,0,d_2T)\boldsymbol{x}(0) \\
&\quad +\boldsymbol{I}(s_1,1,0,d_2T))) + \boldsymbol{I}(s_1,0,d_2T,T), \\
(1,s_2) \to (0,s_2): \quad \boldsymbol{x}(T) &= \boldsymbol{\Phi}(0,s_2,d_1T,T)((\boldsymbol{\Phi}(1,s_2,0,d_1T)\boldsymbol{x}(0) \\
&\quad +\boldsymbol{I}(1,s_2,0,d_1T))) + \boldsymbol{I}(0,s_2,d_1T,T), \\
(1,1) \to (1,0) \to (0,0): \quad \boldsymbol{x}(T) &= \boldsymbol{\Phi}(0,0,d_k,T)(\boldsymbol{\Phi}(1,0),d_lT,d_kT(\boldsymbol{\Phi}(1,1,0,d_lT)\boldsymbol{x}(0) \\
&\quad +\boldsymbol{I}(1,1,0,d_lT)) + \boldsymbol{I}(1,0,d_lT,d_kT)) + \boldsymbol{I}(0,0,d_kT,T) \\
(1,1) \to (0,1) \to (0,0): \quad \boldsymbol{x}(T) &= \boldsymbol{\Phi}(0,0,d_k,T)(\boldsymbol{\Phi}(0,1),d_lT,d_kT(\boldsymbol{\Phi}(1,1,0,d_lT)\boldsymbol{x}(0) \\
&\quad +\boldsymbol{I}(1,1,0,d_lT)) + \boldsymbol{I}(0,1,d_lT,d_kT)) + \boldsymbol{I}(0,0,d_kT,T)
\end{aligned}$$

Here $k \in [1,2], l = [1,2] - k$. Since these functions are not expressible in closed form, it is difficult to see the character of the map. In the next section we argue that this map should have discontinuities.

4. Bifurcation Analysis

The bifurcation diagram shown in Fig. 4 shows a series of bifurcations happening in a rather narrow space of the demanded current I_{ref1}. In order to improve the visibility, we present another bifurcation diagram for $V_{\text{in2}} = 6$ V (instead of $V_{\text{in2}} = 7$ V) in Fig. 5, where only 3 bifurcations are observed. In this diagram, in the range $I_{\text{ref1}} = [0.2 - 0.8]$ we notice a period incrementing cascade where period-3, period-4, and period-5 orbits occur sequentially with overlapping ranges of occurrence as the parameter is reduced. Such *period incrementing cascade* is a specific feature of discontinuous maps [Avrutin *et al.*, 2007].

In Fig. 5 we see that the period-5 orbit exists from 0.2 A until 0.333 A, period-4 from 0.262 A until 0.61 A and period-3 from 0.474 A until 0.8 A. As a typical example, consider the period-4 orbit and let look at the points of its birth and death. The corresponding waveforms are given in Figs. 6 and 7.

It is known that in a peak current mode boost converter, a border collision bifurcation occurs when the inductor current reaches the reference current exactly at a clock instant. Figs. 6 and 7 show that in this system also the events are border collision, as $i_{L_2} = I_{\text{ref2}}$ at some clock instants shown in the figure. But there is a marked difference in the nature of these border collisions.

In order to appreciate the difference, first consider a simple (one phase) boost converter under peak current mode control. In that system the load current is always less than the inductor current and the output voltage is always greater than the input voltage. Hence during the OFF interval, (a) $i_L - v_c/R$ is always positive and therefore the output voltage increases and (b) since $V_{\text{in}} - v_c < 0$, the inductor current drops. Moreover, discrete time modeling of such a converter leads to a nonsmooth but *continuous* map. To

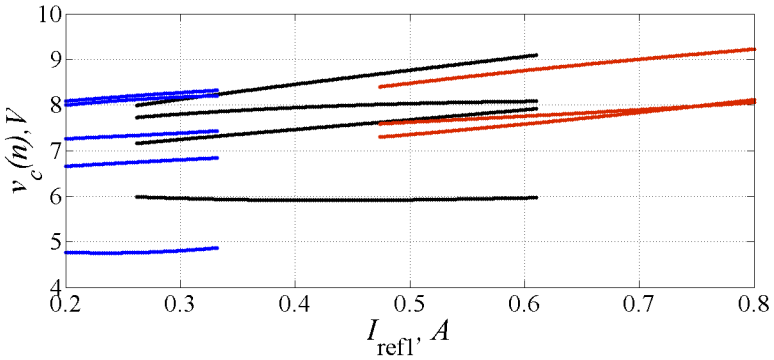

Fig. 5. Bifurcation diagram showing the stable orbits for $V_{in2}=6$ V, $V_{ref}=12$ V, when the sampled values of v_c are plotted. The red trace corresponds to period-3, the black to period-4, and the blue to period-5 orbit. (color online.)

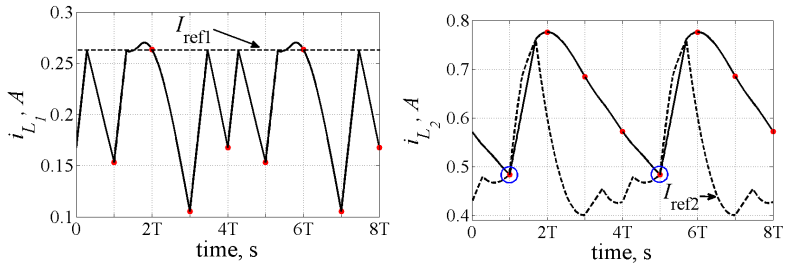

Fig. 6. Current responses for the start of period-4 at $I_{ref1}=0.262$ A. The circles (blue) indicate border-collision. The dots (red) indicate sampled point at the end of each period. (color online.)

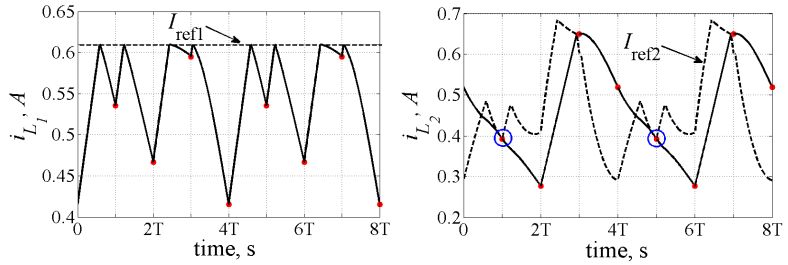

Fig. 7. Current responses for the end of period-4 at $I_{ref1}=0.61$ A. The circles (blue) indicate border-collision. The dots (red) indicate sampled point at the end of each period. (color online.)

see this, consider two cases where the current i_L reaches I_{ref} just before and just after a clock instant. If i_L reaches I_{ref} just before the clock instant, the switch turns OFF, immediately to be turned ON at the clock instant. If i_L reaches I_{ref} just after the clock instant, the switch will remain ON, and will turn OFF as i_L reaches I_{ref}. In both cases the value of i_L would be very close to I_{ref} at the clock instant, and the switch would be OFF for the whole clock period. As a result, the two values of i_L at the next clock instant would be very close to each other, leading to the map being continuous at the points of nonsmoothness.

In contrast, in our dual input boost converter, these two properties do not always hold. As there are two branches feeding the same load, it is possible that the load current is greater than one of the inductor currents and hence $i_L - v_c/R < 0$. This implies that there are clock cycles where the output voltage decreases even less than V_{in}. This can be seen in Fig. 8 where v_c goes below V_{in2}. Furthermore, because $v_c - V_{in2} < 0$ during the OFF interval the current increases and therefore the inductor current exceeds the demanded current despite it being controlled by a peak current controller. This can be clearly seen in Figs. 6 and 7. The final piece of information that is needed in order to completely understand the nature of these bifurcations is that the demanded current of the second phase at the beginning of each clock signal is increasing faster than the inductor current i_{L_2}.

Now it is possible to explain why the border collisions that appear in our system are a landmark of a discontinuous map. To do that, consider two situations in such a converter, where the current i_{L_2} is just above and just below I_{ref2} at a clock instant. In the first case the switch would turn OFF and would remain OFF for the rest of the clock period. In the second case the switch would turn ON, but since $dI_{\text{ref2}}/dt > di_{L_2}/dt$, the switch OFF condition will not materialize in a short while. The switch will turn OFF only after the slope of I_{ref2} changes sign following a switching in the first phase. Thus, the evolution of the state starting from two arbitrarily close initial conditions will proceed along completely different courses, and will end up in widely separated values in the next clock instant. This is the setting that leads to the map being discontinuous.

The waveforms shown in Figs. 6 and 7 satisfy this description. Therefore the extremities of the ranges of occurrence of the period-4 orbit are marked by border collision events where the map function is discontinuous. This causes the disappearance of the orbits and hard transitions between them at the critical parameter values.

Notice that during the period when v_c drops below one of the input voltages, there is a mismatch between the power absorbed from the source, and that delivered to the load. In order to ensure energy balance over the whole period of the waveform, the excess power taken from the source during that clock cycle has to be released to the load over a few clock cycles during which the second phase remains OFF. As the bifurcation parameter is varied, the number of clock cycles necessary to release this energy also changes. That is why, as I_{ref1} reduces, when the period-4 orbit goes out of existence due to a border collision, a period-5 orbit comes into existence. This is the reason behind the cascade with period increment of 1.

This mechanism described above is true for most of the appearances and disappearances observed in Fig.4 and 5, but there are exceptions. For example, for the period-3 orbit, calculation of eigenvalues shows that it goes through a flip bifurcation and becomes unstable at $I_{\text{ref1}} = 0.474$ A. Its eigenvalues are $-0.9967, -0.1937, -0.0162$ and at $I_{\text{ref1}} = 0.473$ A they become $-1.0021, -0.1925, -0.0162$. The period-6 orbit resulting from this period doubling bifurcation diverges instantly, hits a border, and disappears. That is why it is not seen in Fig. 5.

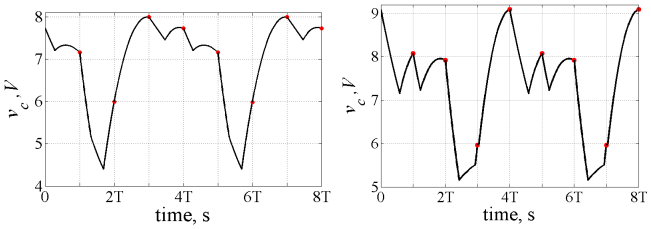

Fig. 8. Voltage responses for $I_{\text{ref1}} = 0.262$ A and $I_{\text{ref1}} = 0.61$ A

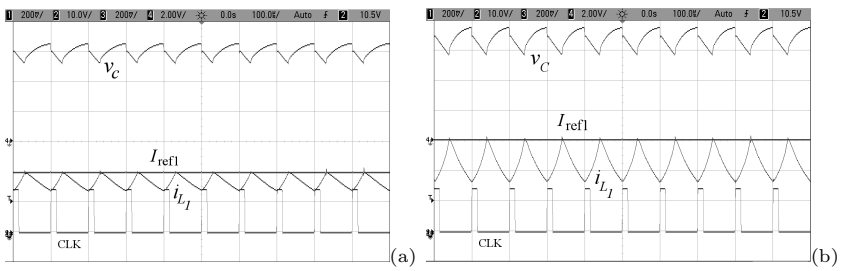

Fig. 9. Experimental waveforms of the period-1 orbit for (a) $I_{\text{ref1}} = 0.4$ A and (b) $I_{\text{ref1}} = 0.6$ A. The clock signal is denoted by CLK.

5. Experimental Validation

In order to validate the aforementioned results an experimental setup was fabricated and was tested with the same parameters (given in the caption of Fig. 2) that were used in the simulation except for a small mismatch in inductors $L_1 = 1.51$ mH, $L_2 = 1.48$ mH (these cannot be made exactly to specification). The nominal period-1 waveforms with the variation of $I_{\rm ref1}$ are shown in Fig. 9.

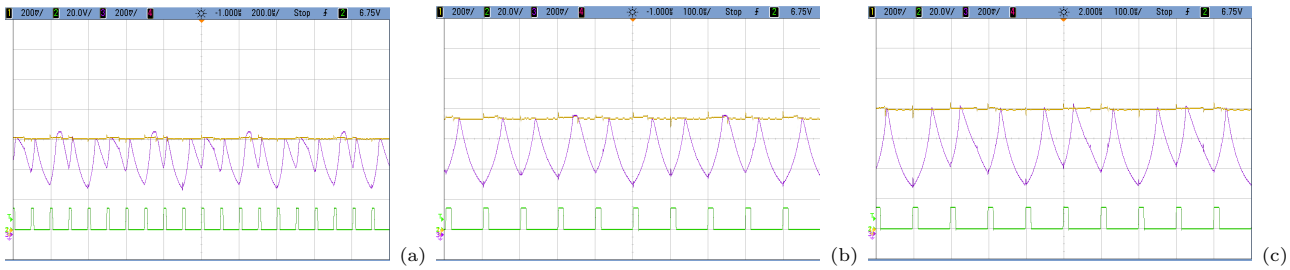

(a) (b) (c)

Fig. 10. Experimental waveforms of i_{L_1} (a) period-5 at $I_{\rm ref1} = 0.60$ A, (b) period-4 at $I_{\rm ref1} = 0.76$ A, and (c) period-3 at $I_{\rm ref1} = 0.80$ A.

To validate the observations in Figs. 6-7, we now change $V_{\rm in2}$ from 7 V to 6 V (with $V_{\rm in1} = 5$ V fixed). Fig. 10 shows the waveforms showing the occurrence of period-5, period-4, and period-3 orbits for different values of $I_{\rm ref1}$, as predicted in the last section. The minor differences can be attributed to the non-ideality of the components like the ESR of the inductors and capacitors, the forward voltages of the MOSFETS and diodes, snubbers and delay circuits in the switch network, etc.

6. Conclusions

In this paper we have considered a dual-input boost converter, and investigated its dynamical behavior. We show that the system can exhibit abrupt changes in periodicity as a parameter is varied, and different classes of bifurcations—smooth, non-smooth but continuous, and non-smooth and discontinuous—are found to occur in the same system. We have then demonstrated why the discrete time model of the system should lead to a discontinuous map. The application of discontinuous maps in the analysis of power electronic systems is very rare. Indeed, the theory of discontinuous maps has been developed only for one- and two-dimensional systems, and the demonstration of the existence of such a map in a three-dimensional system may provide the motivation for the development of the theory of discontinuous maps in higher dimensions.

Acknowledgements

This paper was supported by the NSTIP strategic technologies program in the Kingdom of Saudi Arabia-Project No.(12-ENE3049-03). The authors also, acknowledge with thanks the Science and Technology Unit, King Abdulaziz University for technical support.

References

Avrutin, V., Schanz, M. & Banerjee, S. [2007] "Codimension-three bifurcations: Explanation of the complex one-, two-, and three-dimensional bifurcation structures in nonsmooth maps," *Physical Review E* **75**, 066205.

Banerjee, S. & Chakrabarty, K. [1998] "Nonlinear modeling and bifurcations in the boost converter," *IEEE Transactions on Power Electronics* **13**, 252–260.

Banerjee, S., Parui, S. & Gupta, A. [2005] "Dynamical effects of missed switching in current-mode controlled dc-dc converters," *IEEE Transactions on Circuits and Systems II* **461**, 649 – 654.

Banerjee, S. & Verghese, G. C. (eds.) [2001] *Nonlinear Phenomena in Power Electronics: Attractors, Bifurcations, Chaos, and Nonlinear Control* (IEEE Press, New York).

Chen, Y., Tse, C. K., Wong, S. C. & Qiu, S.-S. [2007] "Interaction of fast-scale and slow-scale bifurcations in current-mode controlled dc/dc converters," *International Journal of Bifurcation and Chaos* **17**, 1609–1622.

di Bernardo, M., Budd, C., Champneys, A. R. & Kowalczyk, P. [2008] *Piecewise-smooth Dynamical Systems* (Springer-Verlag, London).

El Aroudi, A., Rodriguez, E., Leyva, R. & Alarcon, E. [2010] "A design-oriented combined approach for bifurcation prediction in switched-mode power converters," *Circuits and Systems II: Express Briefs, IEEE Transactions on* **57**, 218–222.

Giaouris, D., Banerjee, S., Imrayed, O., Mandal, K., Zahawi, B. & Pickert, V. [2012] "Complex interaction between tori and onset of three-frequency quasi-periodicity in a current mode controlled boost converter," *Circuits and Systems I: Regular Papers, IEEE Transactions on* **59**, 207 –214.

Hamill, D. C. & Deane, J. H. B. [1992] "Modeling of chaotic dc-dc converters by iterated nonlinear mappings," *IEEE Transactions on Power Electronics* **7**, 25–36.

Jain, P. & Banerjee, S. [2003] "Border collision bifurcations in one-dimensional discontinuous maps," *International Journal of Bifurcation and Chaos* **13**, 3341–3352.

Kapat, S., Banerjee, S. & Patra, A. [2010] "Discontinuous map analysis of a dc-dc converter governed by pulse skipping modulation," *IEEE Transactions on Circuits and Systems–I* **57**, 1793 –1801.

Kassakian, J. G., Schlecht, M. F. & Verghese, G. C. [1991] *Principles of Power Electronics* (Springer, Reading).

Kuznetsov, Y. A. [2004] *Elements of Applied Bifurcation Theory* (Springer, New York, USA).

Ohata, T. & Saito, T. [2013] "Stability of multi-phase synchronization in parallel dc-dc boost converters with wta switching," *IECON2013*.

Rakshit, B., Apratim, M. & Banerjee, S. [2010] "Bifurcation phenomena in two-dimensional piecewise smooth discontinuous maps," *Chaos* **20**, 033101.

Shi, C., Miller, B., Mayaram, K. & Fiez, T. [2011] "A multiple-input boost converter for low-power energy harvesting," *Circuits and Systems II: Express Briefs, IEEE Transactions on* **56**, 845–849.

Spinu, V., Athanasopoulos, N., Lazar, M. & Bitsoris, G. [2012] "Stabilization of bilinear power converters by affine state feedback under input and state constraints," *Circuits and Systems II: Express Briefs, IEEE Transactions on* **59**, 520–524.

Suto, Z., Masada, E. & Nagy, I. [2009] "Discontinuous iterated map model of bifurcation phenomena in dtc drives," *Electrical Machines and Systems, 2009. ICEMS 2009. International Conference on*, pp. 1–6.

Tse, C. K. [2003] *Complex Behavior of Switching Power Converters* (CRC Press, Boca Raton, USA).

Van der Broeck, H. & Tezcan, I. [2006] "1 kw dual interleaved boost converter for low voltage applications," *Power Electronics and Motion Control Conference, 2006. IPEMC 2006. CES/IEEE 5th International*, pp. 1–5.

Xiong, X., Tse, C. & Ruan, X. [2013] "Bifurcation analysis of standalone photovoltaic-battery hybrid power system," *Circuits and Systems I: Regular Papers, IEEE Transactions on* **60**, 1354–1365.

Yuan, G. H., Banerjee, S., Ott, E. & Yorke, J. A. [1998] "Border collision bifurcations in the buck converter," *IEEE Transactions on Circuits and Systems-I* **45**, 707–716.

Zhao, Y., Feng, J. & Tse, C. [2009] "Stability analysis of periodic orbits of nonautonomous piecewise-linear systems by mapping approach," *Circuits and Systems II: Express Briefs, IEEE Transactions on* **56**, 845–849.

Zhou, L.-W., Zhu, B.-X. & Luo, Q.-M. [2012] "High step-up converter with capacity of multiple input," *Power Electronics, IET* **5**, 524–531.

Zhusubaliyev, Z. T. & Mosekilde, E. [2003] *Bifurcations and Chaos in Piecewise-Smooth Dynamical Systems* (World Scientific, Singapur).